ELSEVIER

Polymer 44 (2003) 623–633

polymer

www.elsevier.com/locate/polymer

Multiple melting behaviour of poly(ethylene terephthalate)

Y. Kong, J.N. Hay*

Metallurgy and Materials, The School of Engineering, The University of Birmingham, P.O. Box 363, Edgbaston, Birmingham B15 2TT, UK

Received 15 July 2002; received in revised form 31 October 2002; accepted 4 November 2002

Abstract

Differential scanning calorimetry (DSC) and temperature modulated DSC (MTDSC) have been used to investigate the melting behaviour of poly(ethylene terephthalate) (PET). Multiple melting endotherms were observed even at high heating rates, e.g. 160 K min^{-1} and these have been attributed to the presence of two different distributions of lamella thickness and re-crystallisation (reorganisation) on heating. This has been confirmed by MTDSC—the presence of endotherms and an exotherm in the reversing component of the heat flow during heating. Examination of the endotherms of samples heating stepwise indicated that further crystallisation took place above the isothermal crystallisation temperature (T_c). Some part of this was associated with lamella thickening and crystal perfecting. The multiple melting endotherms observed are a consequence of the balance between the melting and re-crystallisation and the lamella thickness distribution existing within the sample, prior to heating. The triple melting endotherms observed are attributed to the melting of secondary and primary lamellae produced on crystallisation and to thickened lamellae produced during heating to the melting point.

Keywords: Multiple melting; Poly(ethylene terephthalate); Lamella thickness distribution

1. Introduction

The melting of polymers is different from that of low molar mass materials in that melting generally occurs over a wider temperature range and is greatly dependent on sample thermal history. The presence of multiple melting endotherms as observed by differential scanning calorimetry (DSC) is very common and has been observed with many semi-crystalline polymers, copolymers and blends [1–23]. The phenomenon has been extensively studied but conflicting interpretations have been made. A variety of effects have been invoked to explain the phenomenon, i.e. to the presence of more than one crystallographic forms (polymorphism); to the presence of melting/re-crystallisation and re-melting; to changes in morphology, such as lamella thickening and crystal perfecting; to changes in orientation; and to the effect of molecular weight distribution [1,24,25]. It is more likely that one of these mechanisms alone cannot explain the observation of multiple endotherms.

PET is an important engineering polymer, whose properties are markedly dependent on the degree and quality of crystallinity. PET crystallises over a wide temperature range, and samples crystallised to the same degree of crystallinity at different temperatures have different melting characteristics. These samples frequently exhibit multiple melting endotherms, which depend on the thermal history. Bell et al. [12,26] using differential thermal analysis (DTA), birefringence and dynamic mechanical measurements observed two endotherms and proposed that the lower one represented the melting of imperfect or smaller crystals with partially extended chains, while the higher endotherm was associated with the melting of folded chain crystals. They considered that the folded chain crystals were kinetically preferred and the more extended crystals were thermodynamically preferred [12]. On annealing during heating the folded chain crystals converted to extended chain crystals. On the other hand, Robert [27] attributed the lower melting endotherm to the melting of folded chain crystals and the higher one to bundle-like crystals. Both conclusions were based on the assumption that melting endotherms were directly related to the structures that developed on crystallisation, and the effect of heating scan was not considered. Holdsworth and Turner-Jones later [28] suggested that partial melting and recrystallisation took place during heating to the melt, and observed two endotherms. The lower temperature one was

* Corresponding author. Tel.: +44-121-414-4544; fax: +44-121-414-5232.
E-mail address: j.n.hay@bham.ac.uk (J.N. Hay).

0032-3861/03/$ - see front matter © 2002 Elsevier Science Ltd. All rights reserved.
PII: S0032-3861(02)00814-5

due to the melting of crystals formed at the crystallisation temperature T_c and the other at higher temperature to the melting of crystals produced by annealing on heating. The DSC measured endotherms did not directly reflect the structures produced during isothermal crystallisation. Groenickx et al. [29] came to similar conclusions but they attributed annealing to crystal perfection or lamella thickening on heating.

Zhou and Clough [30] were the first to report three melting endotherms in the melting of PET although others have observed it earlier in other materials [31,32]. They labelled the endotherms I–III in order of increasing melting point. Endotherm I, which normally appeared about 10 K above the crystallisation temperature, was attributed to the melting of the crystals formed during secondary crystallisation, endotherm II to the melting of the crystals formed during primary crystallisation stage and endotherm III to those formed as a result of recrystallisation on heating. This view has also been accepted by others [23,33,34].

More recently, Medellin-Rodriguez et al. [25,35] have studied the melting behaviour of PET by using DSC, polarised light microscopy and SAXS. They found that melting was the morphological reverse of crystallisation with respect to the primary and secondary structures produced. On the basis of the branching lamella model for spherulites, they suggested that spherulites consisted of dominant and subsidiary branches. The subsidiary ones were formed later in the crystallisation and between the dominant branches. Endotherm I was due to the melting of small metastable branches, endotherm II to the melting of main metastable branches, and endotherm III was associated with dominant branches, which underwent some recrystallisation on heating. This is obviously different from the view of Zhou and Clough [30].

MTDSC, in which a small sinusoidal perturbation is superimposed on the conventional linear heating programme, is a useful thermal analysis technique for separating reversing and non-reversing thermal events [36–38]. The temperature and heat flow profiles can be deconvoluted by performing a Fourier transform analysis [39–41] from the rate of change of temperature and heat flow data. This separated the total heat flow, which is equivalent to that obtained by conventional DSC, into reversing and non-reversing components. The non-reversing component is kinetic in nature and can be attributed to non-reversing melting and crystallisation on heating. Using a quasi-isothermal model, Okazaki and Wunderlich [42] found that locally reversible melting and non-reversing crystallisation existed on heating PET to the melting point largely due to molecular nucleation.

Conventional DSC and MTDSC have been used to study the melting behaviour of PET in this paper in an attempt to resolve some of these apparent differences in the assignment of the multiple endotherms.

2. Experimental

Poly(ethylene terephthalate) (PET) was obtained from DuPont, USA, as moulding pellets. It has a number average molecular weight of 19.6 kg mol^{-1} and weight average molecular weight of 36.4 kg mol^{-1}. The PET was dried in vacuum at 373 K for 12 h. prior to moulding into $100 \times 100 \times 1.0$ mm^3 plaques at 553 K (2 min at a pressure of 7.5 MN m^{-2}). The plaques were quenched into ice/water to obtain amorphous samples, as determined by DSC and wide angle X-ray diffraction (WAXD). The same procedure was used to prepare the thin film, 50–70 μm thick.

A Perkin–Elmer differential scanning calorimetry, DSC-2, interfaced to a PC and operating under a nitrogen flow of 20 cm^3 min^{-1} was used to determine the melting characteristics of PET. Samples were cut directly from the moulded sheets using a weight of 10 ± 0.05 mg. Thin film samples were less than 1.0 mg. An empty aluminium pan plus lid was used as reference. The DSC temperature was calibrated from the melting point of ultra-pure materials; stearic acid, indium, tin and lead at heating rates of 20, 10, 5 and 2.5 K min^{-1} and then extrapolated to zero heating rate. For isothermal crystallisations, the samples were heated to above the melting point at 160 K min^{-1}, kept for 3 min to erase the previous thermal history and then cooled to the crystallisation temperature at 160 K min^{-1}. In measuring the melting characteristics samples were heated at 10 K min^{-1} without further cooling.

In the modulated temperature DSC the Perkin–Elmer DSC-2 was adapted to apply a sinusoidal modulation on the linear temperature ramp; details are described elsewhere [43]. A multifunctional PC interface card with several digital to analogue (D/A) and analogue to digital (A/D) converters was used to measure the temperature and heat flow vs. time, as well as being used to generate a DC voltage following a sinusoidal time dependence. This was superimposed on the temperature control voltage. Temperature and enthalpy calibrations were carried out as with convention DSC. A linear heating rate of 2.5 K min^{-1}, modulation period 60 s and temperature amplitude ± 1.0 K was selected. Both the heating and cooling response of the DSC were symmetrical under these conditions.

3. Results and discussion

3.1. The melting behaviour of bulk PET samples

The DSC response of PET samples crystallised isothermally at different temperatures is shown in Fig. 1. To prevent further crystallisation occurring on cooling, the samples were heated from the crystallisation temperature to the temperature of the last trace of crystallinity. Three melting endotherms were observed, namely I–III with increasing temperature, respectively, in samples crystallised at temperatures from 448 to 473 K. In samples crystallised

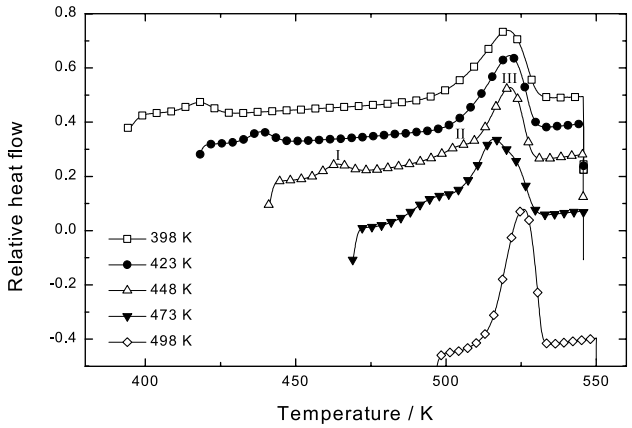

Fig. 1. DSC analyses of the melting of PET. Samples heated immediately after crystallised for 2 h.

below 448 K two endotherms were present, and crystallised at 498 K and above only one. The temperature corresponding to the maximum in the rate of melting of endotherm I, T_{m1}, increased linearly with crystallisation temperature, Fig. 2, indicating that the lamella thickness increased with crystallisation temperature, consistent with nucleation control. Whereas the temperature corresponding to the last trace of melting was independent of the crystallisation temperature below 473 K suggesting that it was due to the melting of lamellae not produced at the crystallisation temperature.

PET samples were also crystallised to different extents at various temperatures from 423 to 498 K. Their melting endotherms are shown in Fig. 3a–e. Again to prevent further crystallisation on cooling they were heated from the crystallisation temperature to melt. Endotherm I was observed to shift progressively to higher temperatures and increased in size with increasing time and crystallinity, Fig. 4, at all crystallisation temperatures. Samples crystallised at 423 K and below showed two endotherms and the final endotherm was constant regardless of time. Samples crystallised at 448 K exhibited three endotherms, I–III, Fig. 3b. II was smaller than III, but it increased in size with

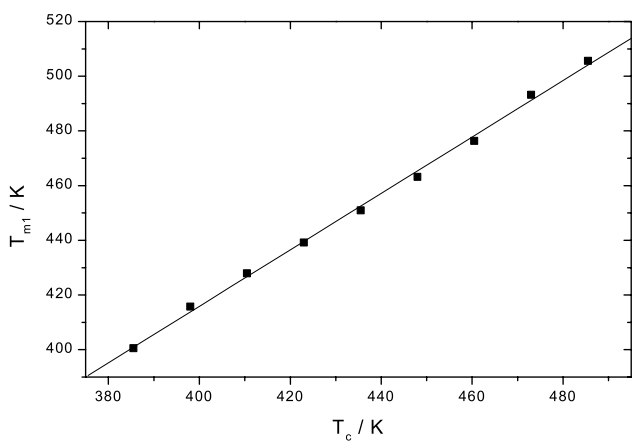

Fig. 2. Endotherm I peak temperature T_{m1} vs. T_c. PET samples crystallised for 2 h at T_c.

increasing crystallisation time. The temperature of the last trace of crystallinity of III was also invariant with time.

Samples crystallised at 473 K also showed three endotherms. The temperature range of I increased with time while that of III remained constant, and eventually merged with II and III. Endotherm II also increased with crystallisation temperature, and it initially developed as a shoulder but progressively merged with III with time and increasing crystallisation temperature. Initially samples crystallised at 483 K displayed only one endotherm which did not shift to higher temperature with increasing time although there was some evidence of a minor endotherm being present as a shoulder, see insert in Fig. 3d. This was more apparent at longer times. The DSC analyses of PET samples crystallised at 498 K are shown in Fig. 3e. A single endotherm developed with time and crystallinity, which moved to higher temperatures and became sharper.

At each temperature the T_{m1} values increased linearly with the logarithm of the crystallisation time, t, as can be seen in Fig. 4. This logarithmic time dependence is conventionally associated with secondary crystallisation [44,45] and endotherm I also developed at the same time as the secondary process in that it was observed after the primary had been well established [14]. Endotherm I would appear to be due to the melting of secondary lamellae. These are attributed to the crystallisation of amorphous material between the primary lamellae, which are laid down first during isothermal crystallisation. Since endotherm II is observed from the onset of crystallisation, it is attributed to the melting of these primary lamellae. The increase in T_{m1} with time and crystallisation temperature is due either to increased crystal perfection or to thickening of the lamellae. Alfonso et al. [45] have drawn similar conclusions. The dependence of the temperature corresponding to the last trace of crystallinity, T_m, on the crystallisation time is shown in Fig. 5. With the exception of samples crystallised at 498 K, T_m was independent of time and decreased with increasing crystallisation temperature. We attribute III to the melting of primary lamellae, which have thickened on heating. This is presumed to involve chain extension of the chains in the primary lamellae along the thickness direction. In samples crystallised at 498 K the temperature corresponding to the last trace of crystallinity increased with crystallisation time, suggesting that this is due to primary lamellae which have not chain extended on heating. They are sufficiently stable not to melt and re-crystallise on heating.

To elucidate this interpretation further, PET was crystallised at 473 K for 1 h and then immediately heated at a variety of different rates in an attempt to eliminate re-crystallisation effects. The endotherms can be seen in Fig. 6a. Three endotherms are present at 2.5 and 5 and two at 10 K min^{-1} and higher heating rates. Endotherms I and II are present in all the samples but with increasing rates of heating less time becomes available for re-crystallisation and the ratio of the areas of endotherm III to II drops.

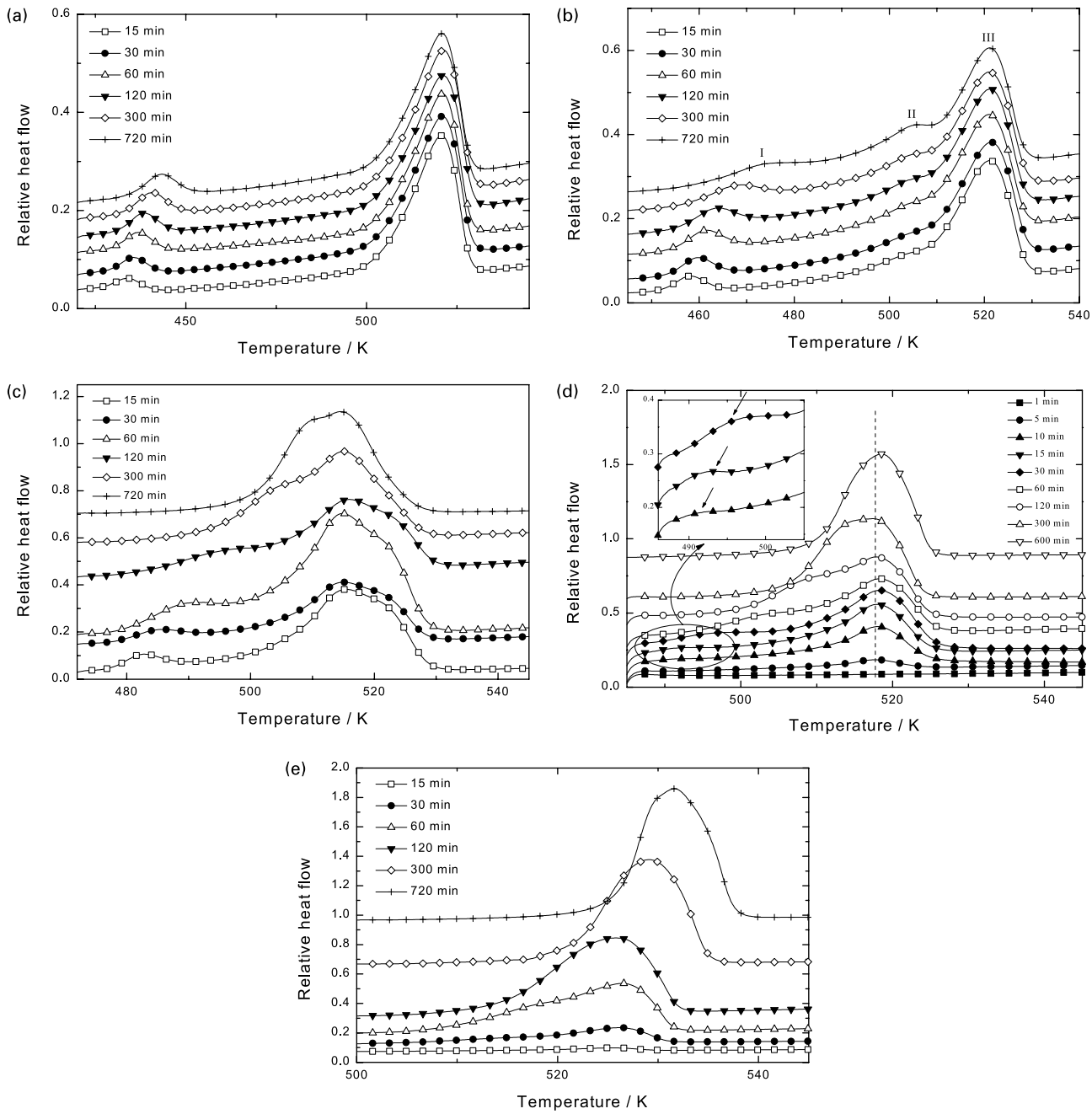

Fig. 3. DSC analyses of the melting of PET. (a) Samples crystallised at 423 K for different times; (b) samples crystallised at 448 K for different times; (c) samples crystallised at 473 K for different times; (d) samples crystallised at 483 K for different times; (e) samples crystallised at 498 K for different times.

Finally, endotherm III disappears with an apparent shift to lower temperatures. Because of the different heating rates, the temperature in Fig. 6a has been corrected for the different thermal lags. These were measured from observed differences in the glass transition temperatures, T_g of the specimens at 2.5–40 K min^{-1}, respectively. Measurements were made on a standard glass produced at a standard cooling rate. On correcting for thermal lag, the temperature corresponding to the start of melting was the same for each sample but T_{m1} increased with increasing heating rate. The melting temperature of endotherm II was almost constant but the temperature corresponding to the last trace of melting decreased with increasing heating rate because of the change from endotherm III to II.

PET samples crystallised at 498 K for 2 h exhibited one endotherm at the higher heating rates, and two endotherms, one as a shoulder, at the lower heating rates. This can be seen in Fig. 6b. The temperature corresponding to the last trace of melting was observed to be independent of heating rate but melting generally occurs at a lower temperature with increasing heating rate. In general, increasing heating rate allows less time for

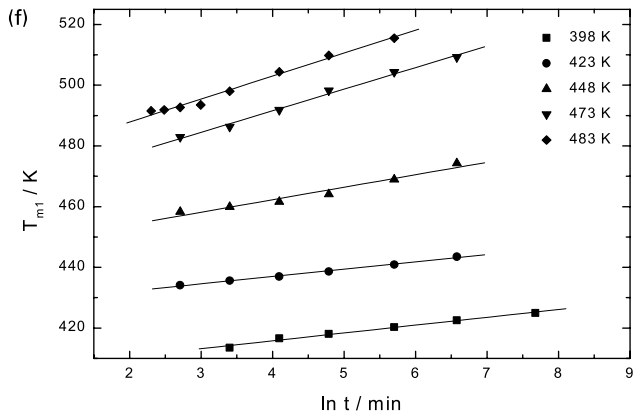

Fig. 4. The dependence of T_{m1} on crystallisation temperature and time.

re-organisation of the crystals to occur and the melting occurs at a lower temperature range.

In DSC, heat flow can be divided into two components [46]—one due to the underlying heat capacity change and the other to changes in crystallinity with temperature,

$$dH/dt = C_p\beta = [C_{p,c}X_c + C_{p,a}(1 - X_c)]\beta - \left[\Delta H_f^0 \frac{dX_c}{dT}\right]\beta \quad (1)$$

where $C_{p,c}$ and $C_{p,a}$ are the heat capacities of the crystalline and amorphous material, respectively, X_c the weight fraction crystallinity, ΔH_f^0 the heat of fusion of 100% crystalline material at T, dX_c/dT the rate of the change of crystallinity with temperature and β the heating rate. Obviously, if dX_c/dT is equal to zero only changes in specific heat of the samples with temperature are measured. This is the case observed with sapphire, Fig. 7, in which the relative heat flow was linear with temperature in line with the specific heat. The melting endotherms of samples crystallised at 423 K for 30 min are shown in Fig. 8. On continuous heating from the crystallisation temperature, trace A, two endotherms were observed at about 435 and 520 K. Between these two endotherms it would appear that no melting or crystallisation is occurring. On step heating to

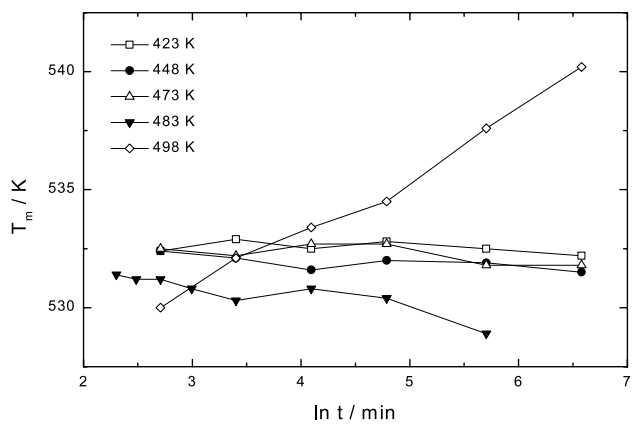

Fig. 5. The dependence of the final melting temperature on crystallisation temperature and time.

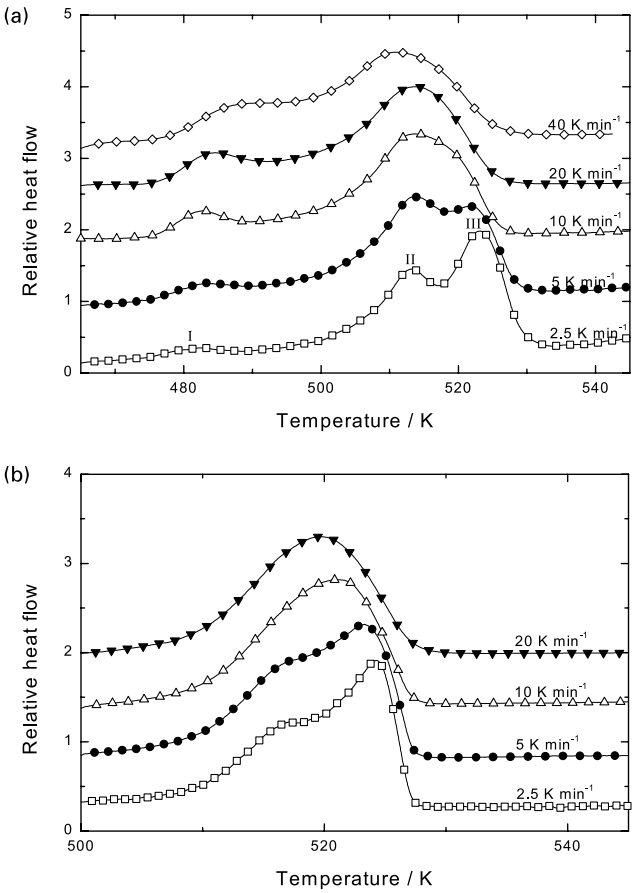

Fig. 6. DSC analyses of the melting of the PET. (a) Samples crystallised at 473 K for 1 h at different heating rates; (b) samples crystallised at 498 K for 2 h at different heating rates.

450 K, above the temperature range of endotherm I, immediately cooling to 30 K lower and reheating to 545 K, endotherm I was observed to shift to a higher temperature. Similarly step heating to other temperatures, traces C to E, endotherm I moves to higher temperatures and to the temperature at which the previous scan stopped. Endotherm II is not altered by this procedure both in temperature range and area of the transition. Obviously

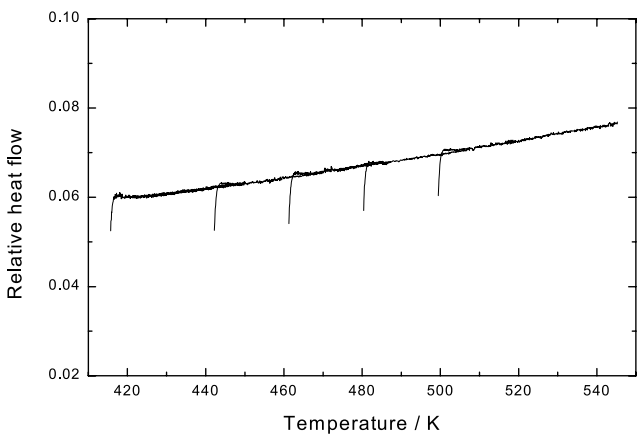

Fig. 7. DSC analyses of sapphire by stepwise heating.

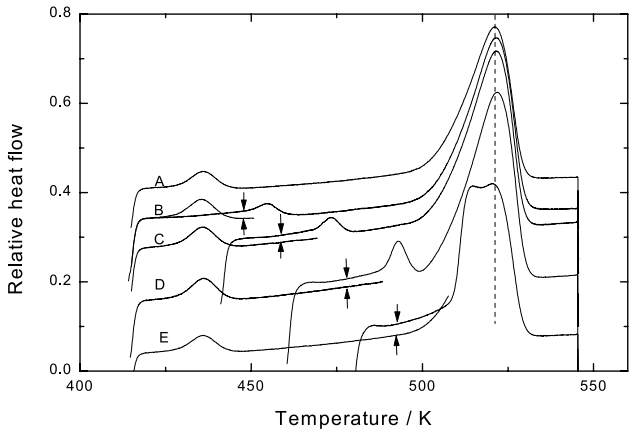

Fig. 8. DSC analyses of the melting of PET. Samples crystallised at 423 K for 30 min. (A) Heating to melt only; (B) heating to 450 K; (C) heating to 470 K; (D) heating to 490 K; (E) heating to 510 K and then cooled by 30 K lower and then heating again immediately.

some re-crystallisation must occur between the two scans but at progressively higher temperatures. Analyses of step heating of samples crystallised at different temperatures were carried out such that after each step the samples were cooled by 10 K at 160 K min^{-1} and then heated immediately at 10 K min^{-1}. The heat flow differences are shown for all the steps in Fig. 9a–c. Clearly melting and then re-crystallisation is taking place on heating and the temperature of endotherm I is dependent on the upper temperature reached in the heating stage.

3.2. The melting of thin films

Fast heating has been shown to be successful in minimising annealing, melting and re-crystallisation of metastable polymer crystals [47] and more successful in determining the melting temperature of the lamellae produced at the crystallisation temperature. However, Medellin-Rodriguez et al. [25] claimed that there were spurious peaks observed on melting, which were associated with fast heating. In the present study, no abnormal spikes or transitions were observed which were additional to the normal endotherms observed at conventional heating rates, as can be seen in Figs. 10 and 11 for both sapphire and PET samples. The DSC was observed to equilibrate after 30 s on first heating independent of heating rate. Normally, as the heating rate increases the thermal lag and temperature gradient across the sample increases due to poor thermal conductivity. To minimise this effect, extremely thin films were used. Using the procedure outlined above, the thermal lag of the film at 160 K min^{-1} was 16 K.

The melting of film samples crystallised at different temperatures but heating at 160 K min^{-1} is shown in Fig. 12. At least two endotherms, I and II, were observed in all the samples except those crystallised at 493 K and above. The lower endotherm I shifted to higher temperatures with increasing crystallisation temperature while the temperature

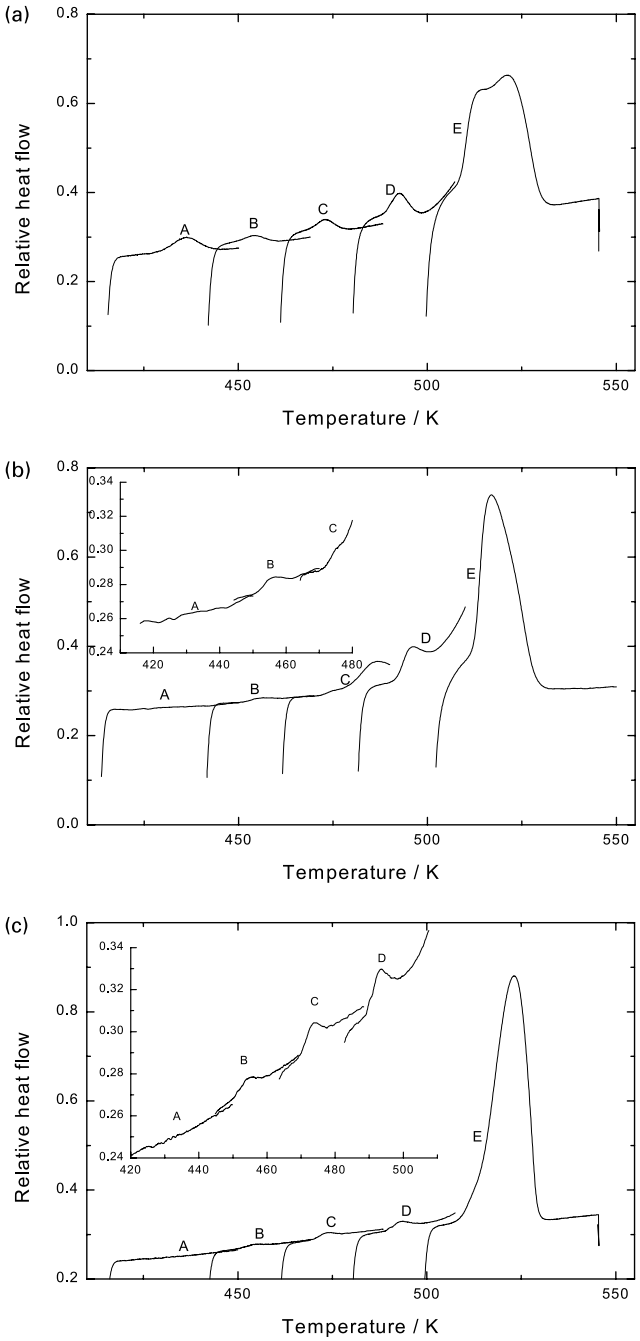

Fig. 9. (a) DSC analyses of the stepwise melting of PET. Sample crystallised at 423 K for 30 min. After each step heating, cooled 10 K and then heated immediately. (A) 415–450 K; (B) 440–470 K; (C) 460–490 K; (D) 480–510 K; (E) 500 K to melt. (b) DSC analyses of the stepwise melting of PET. Samples crystallised at 473 K for 30 min. After each step heating, cooled 10 K and then heated immediately. (A) 415–450 K; (B) 440–470 K; (C) 460–490 K; (D) 480–510 K; (E) 500 K to melt. (c) DSC analyses of the stepwise melting of PET. Samples crystallised at 498 K for 3 h. After each step heating, cooled 10 K and then heated immediately. (A) 415–450 K; (B) 440–470 K; (C) 460–490 K; (D) 480–510 K; (E) 500 K to melt. The rate of cooling 160 K min^{-1} and heating 10 K min^{-1}.

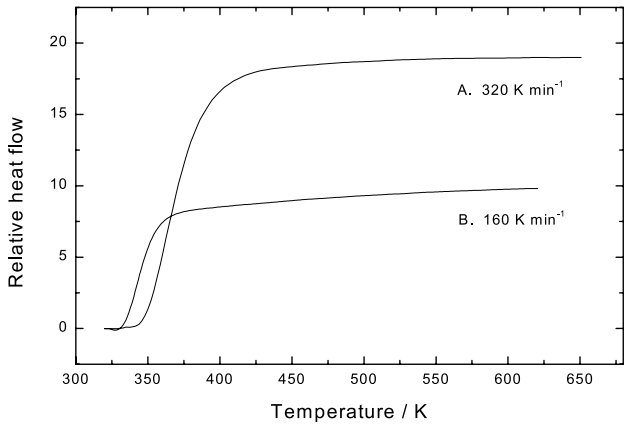

Fig. 10. DSC analyses of sapphire heating at 160 K min^{-1}.

corresponding to the last trace of crystallinity remained constant. Samples crystallised at 453 K showed evidence of a third endotherm as a shoulder on the low temperature side of the second endotherm. The breadth of endotherm II and the drop in the temperature of the maximum rate of melting suggested that this third endotherm was present but had merged with endotherm II. Finally in samples crystallised at 493 K and above, endotherm I merged completely with the second endotherm and a single endotherm was observed. It was apparent that re-crystallisation had taken place in some of the intermediate temperature samples even at such a heating rate.

A comparison was made of the same samples but heated at 20 K min^{-1} in Fig. 12b. A similar trend in the development of the endotherms was observed but in general three endotherms were observed which were reduced to two and then one as first endotherm I and then II shifted to higher temperatures with increasing crystallisation temperature. Eventually they merged into two and then one endotherm. The slower heating rate made the changing pattern of the endotherms more obvious since there was greater time for the reorganisation to take place at lower temperatures, and endotherm II was more differentiated from III. Except for samples crystallised at 503 K, which exhibited one very

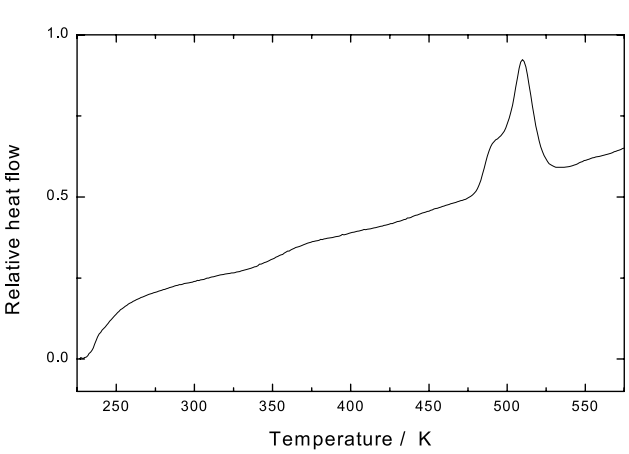

Fig. 11. DSC analysis of melting of PET thin films. Heating rate 160 K min^{-1}.

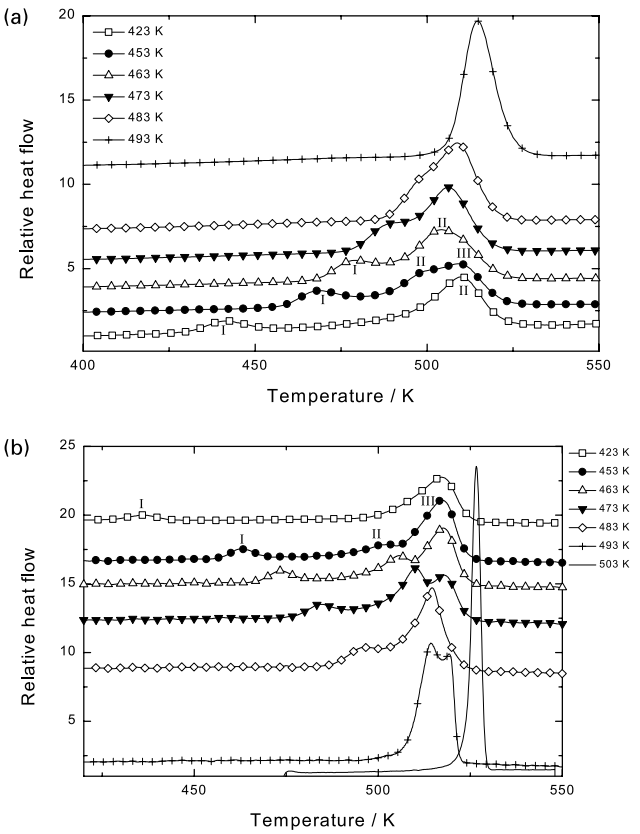

Fig. 12. DSC analysis of the melting of PET thin films. Samples crystallised at different temperatures. (a) Heating rate 160 K min^{-1}; (b) heating rate 20 K min^{-1}.

sharp endotherm in a temperature range above that observed in the other samples, the temperature corresponding to the last trace of crystallinity was independent of crystallisation temperature, indicating that this endotherm was associated with the melting of annealed lamellae.

Three endotherms were observed in the thin films crystallised at 473 K at the different heat rates see Fig. 13. On correcting for thermal lag, the temperature corresponding to the onset of melting was observed to be constant.

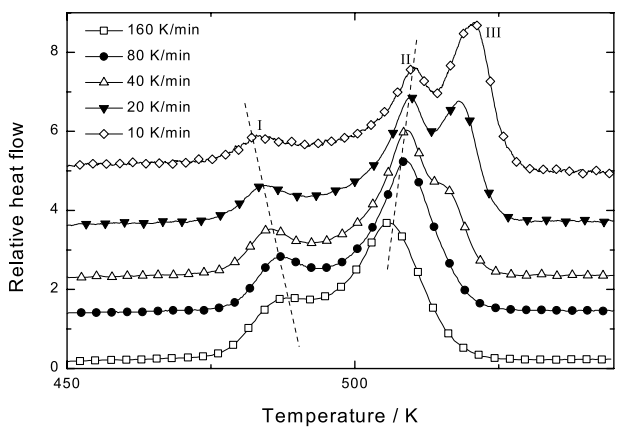

Fig. 13. DSC analysis of the melting PET thin films. Samples crystallised at 473 K for 30 min. Heated at different rates.

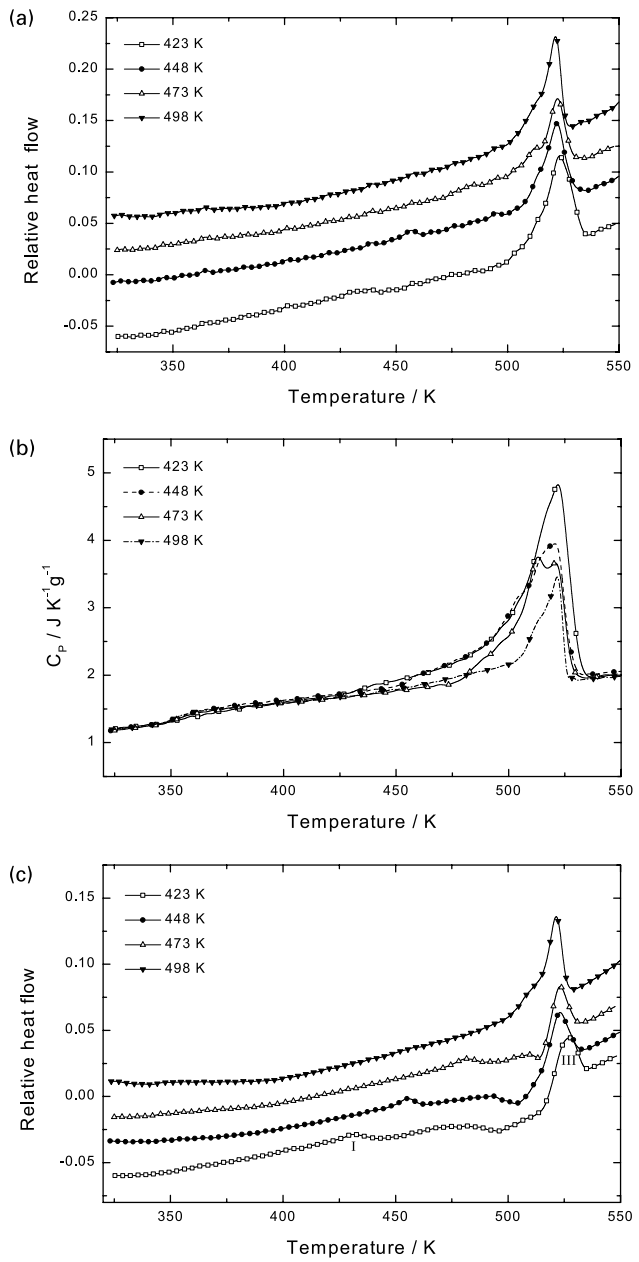

Fig. 14. MTDSC analyses of the melting of PET. (a) Total heat flow of the samples crystallised at various temperatures; (b) reversing heat capacity of the samples crystallised at various temperatures; (c) non-reversing heat flow of the samples crystallised at various temperatures.

However, with increasing heating rate endotherm I increased in area and shifted to higher temperature. Endotherm III gradually decreased in size and disappeared at a heating rate of 80 K min^{-1} and above. Endotherm II shifted slightly to lower temperatures. This is consistent with the above interpretation that endotherm I corresponds to the melting of secondary lamellae and with increasing heating rate melting moves to higher temperature with the reduction in time spent at each temperature. Endotherm II is associated with the melting of primary lamellae while endotherm III to the melting of lamellae, which have thickened or annealed on heating. The size of endotherm II decreases while that of III increases with slower heating rates. With slower rates more time is available for reorganisation of the lamellae and the primary lamellae are disappearing with the production of the thicker more stable lamellae.

3.3. A study of the melting behaviour by MTDSC

In MTDSC the average heat flow measured is equivalent to the conventional DSC signal. Reversing thermal events such as glass transition and partially melting contribute to the reversing signal; while events such as de-ageing, crystallisation, and melting contribute to the non-reversing signal [48,49]. The MTDSC analysis of PET samples crystallised at different temperatures for 1 h are shown in Fig. 14. The average heat flow—temperature plots show slight variations due to the different crystallisation temperatures adopted but a single endotherm with a shoulder is present with a drift to increasing temperature with increasing crystallisation temperature, Fig. 14a. The reversing heat capacities, Fig. 14b, is the same for all the samples up to the crystallisation temperature. Thereafter, they deviate due to the onset of melting, the deviation setting in above the crystallisation temperature. Only one endotherm is present, i.e. III with a low temperature shoulder which is the residue of II. Two endotherms, I and III, are present, Fig. 14c, in the non-reversing heat flow-temperature plots of all the samples. Endotherm I occurs just above T_c and shifts with the crystallisation temperatures. This endotherm is followed by an exotherm that also shifts to higher temperature with increasing T_c. It is not present in samples crystallised at 498 K but I appears as a shoulder of the final endotherm.

Endotherm III, above 515 K, is considered to be an experimental artefact in the non-reversing component arising from a mismatch between the thermal response on heating and cooling while most of the sample is melting. This results in the calorimeter response under the experimental conditions selected no longer being in equilibrium.

MTDSC clearly shows that endotherm I is followed by an exotherm above 480–520 K depending on value of T_c, which is due to some re-crystallisation. This occurs in the same temperature region as endotherm II and is not observed by conventional DSC. Both the melting endotherm and the re-crystallisation exotherm are similar in magnitude, implying that re-crystallisation occurs by the incorporation of the amorphous material produced from the melting of the secondary lamellae.

MTDSC does not clearly distinguish between endotherms II and III since it is a slow heating technique, 2.5 K min^{-1}, and there is sufficient time, by analogy to results presented in Fig. 6a and b, for the primary lamellae to anneal completely.

3.4. Discussion

There is considerable disagreement in the interpretation of multiple melting endotherms in polymers and we have invoked both melting followed by re-crystallisation during heating [16,28] and two separate distributions of lamella thickness [14,50]. From the stepwise heating and MTDSC studies it is clear that melting and recrystallisation take place during the heating even in samples, which have been crystallised at high temperatures. The extent of recrystallisation that occurs depends on the sample history and the experiment conditions selected to heat to the melting point. However, a dual lamella thickness distribution exists within all samples crystallised isothermally. In Fig. 3d and e it can be seen that samples crystallised at 483 and 498 K to a low degree of crystallinity exhibited only one melting endotherm corresponding to endotherm II. With increasing crystallisation time two melting endotherms were observed, indicating that endotherm II appeared earlier in the crystallisation than endotherm I. PET crystallisation at 483 and 498 K has half-lives of 11 and 40 min, respectively, and endotherm I developed only after 10 and 30 min into the crystallisation. This means that the less stable lamellae are not produced at the very beginning of the crystallisation but start to form before primary crystallisation stops. They are clearly associated with the onset of the secondary process. Recently Hsiao et al. [51] observed that the average long period and lamella thickness decreased with time particularly towards the end of the primary crystallisation stage. This decrease is due to the formation of two populations of lamella thickness—primary lamellae, which form initially in the primary crystallisation stage and secondary lamellae, which form towards the end of the primary crystallisation stage and are thinner. This reduces the average value and it is the melting of these, which gives rise to endotherm I.

PET thin film samples, at high heating rates, show two distinct endotherms, I and II, which arise from the two distribution of lamella thickness. At lower heating rates three endotherms are observed. The ratio of the magnitudes of endotherms II and III also changes, endotherm II disappearing at the expense of III at lower heating rates. Accordingly endotherm III is attributed to the melting of thickened primary lamellae either by re-crystallisation and/or by chain extension.

If endotherm I occurs at too high a temperature or if the heating rate is too high there is not sufficient time for re-crystallisation to develop, and endotherm III is absent from the DSC response as can be seen in Fig. 15 where the same samples, A and B, are heated at 20 and 160 K min^{-1}, respectively. Sample A exhibited three endotherms, B two and a sample C crystallised for a longer period of time, only one. The fast heating rate in B did not allow sufficient time for re-crystallisation to occur and endotherm III is absent. The long period of time for the crystallisation of C enabled the secondary lamellae to become more stable, in that the melting temperature increases with logarithm of the time.

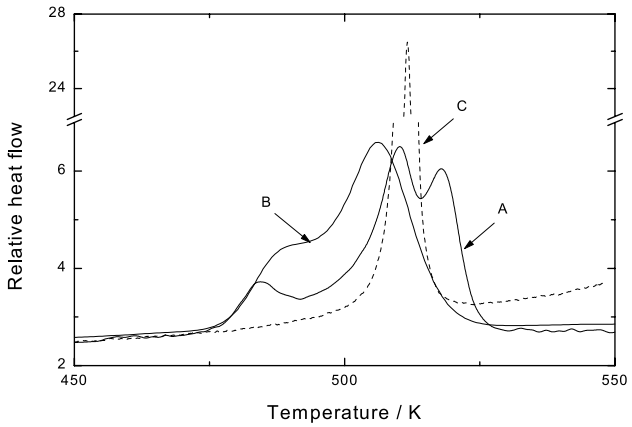

Fig. 15. DSC analyses of the melting of PET thin film. Samples crystallised at 473 K. (A) For 30 min, heating rate 20 K min^{-1}; (B) for 30 min, heating rate 160 K min^{-1}; (C) for 48 h, heating rate 20 K min^{-1}.

Endotherm I merges with II and re-crystallisation cannot take place. Endotherm III is accordingly absent. The presence of one, two or three endotherms is a result of the balance between the primary and secondary crystallisation, their lamella thickness distributions and the extent of melting/re-crystallisation occurring during heating, i.e. heating rate.

If endotherm II reflect the original crystalline lamella thickness, Fig. 16, the equilibrium melting temperature, T_m^0, can be determined using the Hoffman–Week's relationship [52]. The observed melting point T_m is related to T_c by,

$$T_m = T_m^0\left(1 - \frac{1}{\gamma}\right) + \frac{T_c}{\gamma} \quad (2)$$

A linear plot of T_m vs. T_c was observed, as shown in Fig. 17, from which the value of lamella thickening coefficient, γ, was determined to be about 2.0 indicating that the maximum lamella thickness was close to the critical size of the primary nucleus and the measurement of T_m was carried out under equilibrium conditions. No re-crystallisation or crystal perfection could have occurred during

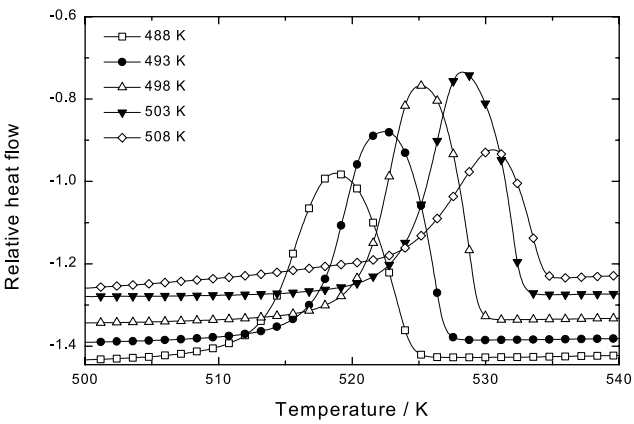

Fig. 16. DSC analyses of the melting of PET. Samples crystallised for 10 h, heating rate 5 K min^{-1}.

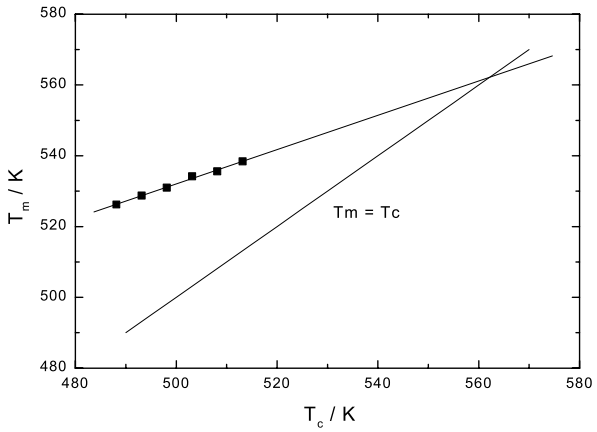

Fig. 17. Hoffman–Weeks' plot for PET. Plot of melting point, T_m, against crystallisation temperature, T_c.

heating. The extrapolated value of T_m^0 was 561 ± 2 K in good agreement with the literature values [23,29].

On heating crystallised samples to temperatures intermediate between endotherms I and II, endotherm I re-appears on cooling to the original crystallisation temperature but I is displaced to higher temperatures, Fig. 8. This increase in the temperature of endotherms has been observed by others [3,30,35] but never fully explained. There can be two apparent reasons for it. One is melting of the secondary lamellae and re-crystallisation at that temperature or on cooling; and the other to annealing of these lamellae as a result of heating to a higher temperature. There is no increase in crystallinity as the two endotherms have similar magnitudes and the secondary lamellae are clearly melting and subsequently re-crystallisation as secondary lamellae at a higher temperature and so increased thickness. There is no evidence of annealing as endotherm II does not shift to higher temperatures.

On first heating endotherm I is always present at the same temperature shown by sample A, Fig. 8. However, on subsequent cooling and heating endotherm I shifts progressively to higher temperatures, samples B–D. Clearly melting is followed by re-crystallisation of the amorphous material produced and the lamella thickness increases with crystallisation temperature. The extent of crystallinity, which develops is limited and the subsequent endotherm is attributable to the melting of secondary lamellae which have thickened as a result of crystallising at a higher temperature. This procedure appears to occur both below and above the crystallisation temperature as can be seen in Fig. 9a–c with samples crystallised at different temperatures. Endotherm I developed either at T_c, or below for samples crystallised at 473 and 498 K, respectively. Heating these samples to various temperatures enabled endotherm I to develop during the heating scan. The size and temperature range varying with the temperature at which the previous scan was stopped. These endotherms are small compared to those developed during isothermal crystallisation, as shown in Figs. 8 and 9a. but reflect the production of secondary lamellae during the temperature scan. It can be seen from Fig. 9a–c that the re-crystallisation takes place close to the temperature at which the first heating was stopped. Finally, at a sufficiently high crystallisation temperature the secondary lamellae produced initially have sufficient stability similar to that of the primary and I and II merge together into one overall endotherm.

4. Conclusions

The melting characteristics of PET samples are very complex depending on the experimental conditions chosen for the measurements, isothermal temperature or non-isothermal crystallisation conditions, thermal history and heating rate. It is confirmed that when two endotherms, I and II, are present that these are due to the presence of a dual lamella thickness distribution produced during crystallisation. Three endotherms have also been observed in the samples crystallised at intermediate super-cooling. The addition endotherm, III, is associated with the melting of the thickest lamellae. These are produced on heating after the melting of the secondary lamellae and by re-crystallisation of the primary lamellae, which leads to chain extension and lamella thickening.

Acknowledgements

One of the authors, Y. Kong, acknowledges the award of a research scholarship from ORS Committee and the Department of Metallurgy and Materials of the University of Birmingham during the tenure of this work. The authors would like to express their appreciation to Mr F. Biddlestone for his technical support and assistance.

References

[1] Wunderlich B, Macromolecular physics, vol. 3. New York: Academic Press; 1976.
[2] Bair HE, Salovey R, Huseby TW. Polymer 1967;8:9.
[3] Harrison IR. J Polym Sci: Polym Phys Ed 1973;11:991.
[4] Feng Y, Jin X, Hay JN. Polym J (Jpn) 1998;30:215.
[5] Vandermiers C, Moulin JF, Damman P, Dosiere M. Polymer 2000;41:2915.
[6] Samuels RJ. J Polym Sci: Polym Phys Ed 1975;(13):1417.
[7] Busfield WK, Blade CS. Polymer 1980;21:35.
[8] Wlochowicz A, Eder M. Polymer 1984;25:1268.
[9] Woo EM, Fu SW. Macromol Chem Phys 1998;199:2041.
[10] Liu T, Petermann J. Polymer 2001;42:6453.
[11] Wang C, Hsu YC, Lo CF. Polymer 2001;42:8447.
[12] Bell JP, Murayama T. J Polym Sci, Part A-2 1969;7:1059.
[13] Tan S, Su A, Yang X, Zhou E. J Appl Polym Sci 2000;77:993.
[14] Chung JS, Cebe P. Polymer 1992;33:2312. see also page 2325.
[15] Mai K, Mei Z, Xu J, Zeng H. J Appl Polym Sci 1997;63:1001.
[16] Blundell DJ. Polymer 1987;28:2248.
[17] Lee Y, Poter RS. Macromolecules 1987;20:1336.

[18] Lattimer MP, Hobbs JK, Hill MJ, Barham PJ. Polymer 1992;33:3971.
[19] Yeh JT, Runt J. J Polym Sci: Polym Phys Ed 1989;27:1543.
[20] Nichols ME, Robertson RE. J Polym Sci: Polym Phys Ed 1992;30: 755.
[21] Groeninckx G, Reynaers H. J Polym Sci: Polym Phys Ed 1980;18: 1325.
[22] Fontaine F, Ledent J, Groeninckx G, Reynaers H. Polymer 1982;23: 185.
[23] Lu XF, Hay JN. Polymer 2001;42:9423.
[24] Hobbs SY, Pratt CF. Polymer 1975;16:462.
[25] Medellin-Rodriguez FJ, Phillips PJ, Lin JS, Campos R. J Polym Sci, Part B: Polym Phys 1997;35:1757.
[26] Bell JP, Dumbleton JH. J Polym Sci, Part A-2 1969;7:1033.
[27] Roberts RC. Polymer 1969;10:117.
[28] Holdsworth PJ, Turner-Jones A. Polymer 1971;12:195.
[29] Groeninckx G, Reynaers H, Berghmans H, Smets G. J Polym Sci: Polym Phys Ed 1980;8:1311.
[30] Zhou C, Clough SB. Polym Engng Sci 1988;28:65.
[31] Booth C, Devoy CJ, Dogson DV, Hillier IH. J Polym Sci, Part A-2 1970;8:519.
[32] Lemstra PJ, Kooistra T, Challa G. J Polym Sci, Part A-2 1972;10:823.
[33] Al Raheil IAM. Polym Int 1994;35:189.
[34] Sauer BB, Kampert WG, Neal Blanchard E, Threefoot SA, Hsiao BS. Polymer 2000;41:1099.
[35] Medellin-Rodriguez FJ, Phillips PJ, Lin JS. Macromolecules 1996;29: 7491.
[36] Reading M, Elliot D, Hill VL. J Therm Anal 1993;40:949.
[37] Gill PS, Sauerbrunn SR, Reading M. J Therm Anal 1993;40:931.
[38] Reading M. Trends Polym Sci 1993;8:248.
[39] Wunderlich B, Jin Y, Boller Y. Thermochim Acta 1994;238:277.
[40] Reading M, Luget A, Wilson R. Thermochim Acta 1994;238:295.
[41] Schawe JEK. Thermochim Acta 1995;260:1.
[42] Okazaki I, Wunderlich B. Macromolecules 1997;30:1758.
[43] Bailey NA, Hay JN. J Thermal Anal 1999;56:1011.
[44] Hoffman JD, Weeks JJ. J Chem Phys 1965;42:4301.
[45] Alfonso GC, Pedemonte E, Ponzetti L. Polymer 1979;20:104.
[46] Mathot VBF, editor. Calorimetry and thermal analysis of polymers. Munich: Hanser; 1994.
[47] Hellmuth E, Wunderlich B. J Appl Phys 1965;36:3039.
[48] Jones KJ, Kinshott I, Reading M, Lacey AA, Nikolopoulos C, Pollock HM. Thermochim Acta 1997;304/305:187.
[49] Scherrenberg R, Mathot V, Hemelrijck AV. Thermochim Acta 1999; 330:3.
[50] Bassett DC, Olley RH, Al Raheil IAM. Polymer 1988;29:1745.
[51] Wang ZG, Hsiao BS, Sauer BB, Kampert WG. Polymer 1999;40: 4615.
[52] Hoffman JD, Weeks JJ. Res Nat Bur Stand 1962;66A:13.